Intercalated liquid-crystalline phases formed by symmetric dimers with an α,ω-diiminoalkylene spacer†

Maja Šepelj,[a] Andreja Lesac,*[a] Ute Baumeister,[b] Siegmar Diele,[b] H. Loc Nguyen‡[c] and Duncan W. Bruce*[d]

Received 30th August 2006, Accepted 11th December 2006
First published as an Advance Article on the web 9th January 2007
DOI: 10.1039/b612517d

Four series of symmetric, dimeric molecules with flexible α,ω-diiminoalkylene spacers have been synthesised and characterised by polarising optical microscopy, differential scanning calorimetry, and X-ray diffraction. The effects on the mesomorphism of the various alkylene spacer (number of methylene units $m = 5$ to 8) as well as the terminal alkoxy chain length ($n = 4$ to 14) on the mesomorphic properties have been studied. The compounds with an even-numbered spacer display, in addition to a nematic phase, various smectic phases whose nature depends on the ratio between the length of the terminal chain and the length of the spacer (n/m). A modulated SmÃ phase was found for the ratio $n/m = 1$ to 1.6 and a SmC/crystal G polymorphism emerges at $n/m > 1.7$. In contrast, all liquid-crystalline dimers with odd-numbered spacers display an intercalated B_6 phase regardless of the chain length. The preference for intercalated structures is discussed based on dipolar considerations following electronic structure calculations using a model molecule.

Introduction

Dimeric liquid crystalline compounds, in which two mesogenic units are linked by a flexible spacer, have attracted considerable attention due to their ability to serve as model compounds for liquid-crystalline polymers and their rich and unusual mesomorphism, which differs from that of the corresponding monomers.[1–4] The conformation and the mesomorphic behaviour of such compounds are influenced significantly by the spacer parity,[3–5] which affects the mutual orientation of the mesogenic units, resulting in a linear conformation for an even number and a bent-shaped motif for an odd number of methylene units if an all-*trans* spacer conformation is assumed. In addition to nematic, smectic A and smectic C phases have been frequently observed for the majority of dimers. Within the smectic phase, dimeric molecules can be considered as adopting one of two plausible arrangements (Fig. 1).[6] In the first (Fig. 1a) the molecules intercalate forming a phase in which terminal chains and the spacers are mixed randomly and the layer spacing is approximately half the molecular length. In the second arrangement (Fig. 1b), the molecules are segregated forming three distinct regions containing mesogenic cores, terminal chains and spacers giving rise to, in effect, a smectic phase in which the layer spacing corresponds to the molecular length. Generally the intercalated structures are typical for non-symmetric dimers (two different mesogenic groups) while the vast majority of symmetric dimers display phases with layer spacings approximately equal to the molecular length.

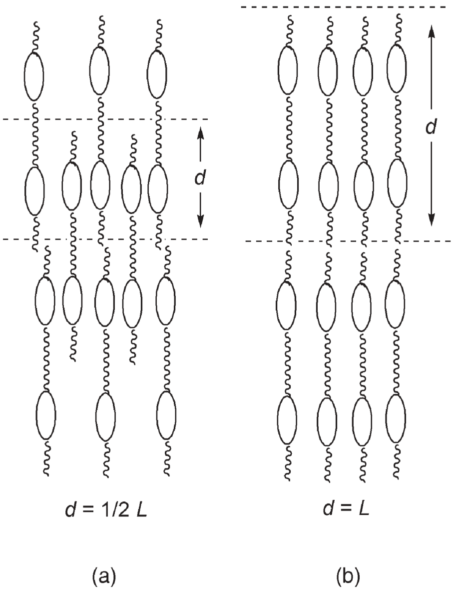

Fig. 1 Diagram to show the two possible arrangements of the dimeric mesogens into layers: (a) intercalated and (b) non-intercalated.

However, Watanabe *et al.*[7–9] observed both types of smectic structures for symmetric dimers: an intercalated arrangement when the length of the terminal chains (n) is smaller than, or comparable to, the length of the spacer (m), and a non-intercalated arrangement when the terminal chains are longer than the spacer. The latter situation becomes very interesting

---

[a] *Ruđer Bošković Institute, Bijenička cesta 54, 10000, Zagreb, Croatia. E-mail: alesac@irb.hr; Fax: +385 14680108*
[b] *Institute of Physical Chemistry, Martin-Luther-Universität Halle-Wittenberg, Mühlpforte 1, 06108, Halle, Germany*
[c] *Department of Chemistry, University of Exeter, Stocker Road, Exeter, UK EX4 4QD*
[d] *Department of Chemistry, University of York, Heslington, York, UK YO10 5DD. E-mail: d.bruce@exeter.ac.uk; Fax: +44 1904 432516*

† Electronic supplementary information (ESI) available: X-ray patterns of **8-12** (Fig. S1) and **6-12** (Fig. S2); χ-scans for the 2D X-ray patterns of the SmC phase of **8-14** (Fig. S3); short take of the powder-like X-ray pattern for the lower temperature monotropic phase of **8-14** (Fig. S4); temperature dependence of θ and FWHM of **7-4**, and χ-scans for the 2D X-ray patterns of **7-4** (Fig. S5); temperature dependence of *d*-values for **7-10** (Fig. S6); colour version of Fig. 4 (Fig. S7). See DOI: 10.1039/b612517d

‡ Present address: Department of Chemistry, University Science Laboratories, South Road, Durham, UK DH1 3LE.

particularly when it arises from dimers with an odd-numbered spacer due to potential antiferroelectric switching properties.[10]

Recently, we described the properties of a range of odd- and even-membered dimeric molecules in which a salicylaldimine core was linked to the alkylene spacer *via* an imino group.[11] The mesomorphic behaviour of the even members was characteristic for symmetric dimers and, depending on the *n*/*m* ratio, they exhibited a nematic and a non-intercalated SmC phase. In contrast, the dimers with an odd-numbered alkylene spacer chain having the same *n*/*m* ratio displayed columnar rectangular phases instead of the non-intercalated SmC phase. In continuation of our investigation of symmetric liquid-crystalline dimers, here we report the mesomorphic properties of a new series of dimeric molecules in which the salicylaldimine core has been replaced by the benzoyloxybenzylidene group. The absence of intramolecular hydrogen bonding both reduces the molecular width and increases the flexibility of the molecule, the latter allowing better inter-mesogen interactions which, in the case of materials with odd-numbered spacers, might lead to the non-intercalated structures with antiferroelectric properties.

Results and discussion

Synthesis

The synthesis of all the compounds was carried out following Scheme 1. All Schiff bases were prepared in good yields of 60 to 80% by addition of α,ω-diaminoalkane to the corresponding aldehyde **3a–f** according to the procedure described previously.[11] The dimers were identified by ^{1}H and ^{13}C NMR spectroscopy, while purity was established by elemental analysis.

Mesomorphism

The mesomorphic behaviour of the new compounds was investigated by polarising optical microscopy, differential scanning calorimetry and X-ray diffraction. The phase transition temperatures and the corresponding enthalpy changes are collected in Tables 1 and 2.

Mesomorphism of 6-*n* and 8-*n*. The data listed in Table 1 reveal that all the dimers with an even-numbered methylene spacer display mesomorphism in accordance with their overall linear shape. In both series, the lower homologues (*n* = 4, 6) exhibit solely a nematic phase, identified by its characteristic schlieren and marbled textures. Increasing the chain length resulted in the additional appearance of various smectic phases. The compounds with intermediate chain lengths showed a smectic A-type phase, established from optical textures obtained on slow cooling of the preceding nematic phase. The texture obtained from the schlieren nematic displayed both focal conic and homeotropic domains. In addition, contact preparation between the smectic A phases of ethyl-(4-ethoxybenzal)-4′-aminocinammate[12] and compounds **6-8**, **8-8** and **8-10** respectively, confirmed complete miscibility of the two phases. Compounds **6-10** and **8-12** represent the highest homologues that display a smectic A phase. On cooling **6-10**, the monotropic phase below the nematic phase displayed a fan-like texture, which closely resembles that of a SmA phase (Fig. 2).

The presence of a smectic A phase is supported by X-ray measurements. The two-dimensional diffraction patterns obtained from samples aligned in a magnetic field clearly showed a two-dimensional modulation of the centred rectangular type with unit cell parameters *a* = 4.3 nm corresponding to the periodicity of the modulation perpendicular to the layer normal and *b* = 5.7 nm corresponding to a layer distance that is in excellent agreement with the molecular length of 5.8 nm as determined from CPK models for a fully stretched molecule (terminal chains and spacer in all-*trans* configuration) measuring along a line connecting the centres of the rings. Thus, the phase is of the type SmÃ, namely a modulated SmA phase (Fig. 3b, Table 3). Estimating the molecular volume in the

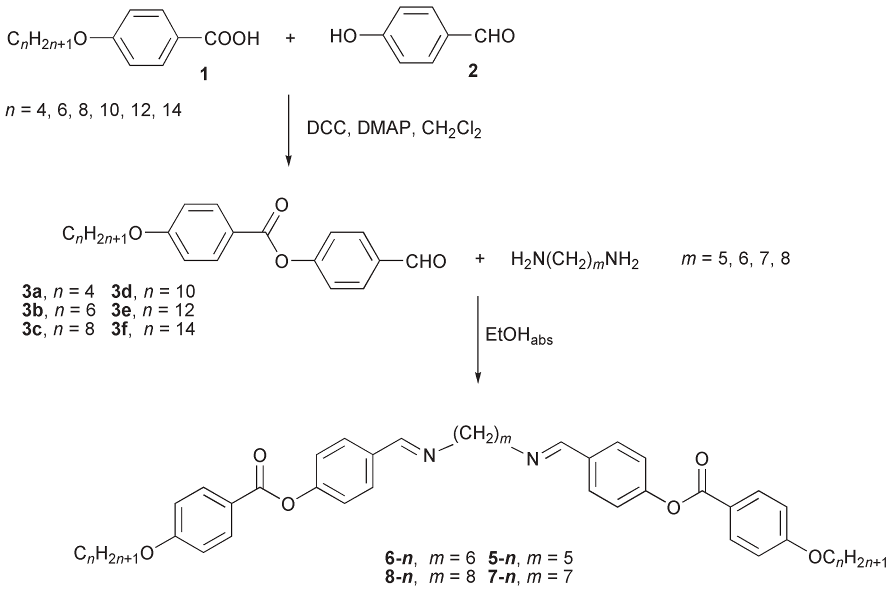

Scheme 1 Synthetic route for the compounds ***m-n*** (*m* = 5,6,7,8, *n* = 4 to 14).

Table 1 Transition temperatures (°C), enthalpies (kJ mol^{-1}) in italics and the dimensionless value of $\Delta S/R$ in square brackets for compounds **6-*n*** and **8-*n***

Dimer	Cr		G		SmB		SmC		SmÃ		N		Iso
6-4	•	164.4 *56.5*[16]									•	182.0 *9.5*[3]	•
6-6	•	141.4 *47.4*[14]									•	164.2 *8.7*[2]	•
6-8	•	133.2 *51.1*[15]							(•	133.2) *−0.9*[0.3]	•	154.3 *9.5*[3]	•
6-10[a]	•	119.6 *51.4*[16]							(•	116.2) *−0.2*[0.1]	•	144.6 *10.8*[3]	•
6-12[b]	•	102.7 *38.8*[12]	(•	94.3) *−6.7*[2]			•	123.9 *2.8*[1]			•	138.4 *11.5*[3]	•
6-14	•	113.8 *64.3*[20]	(•	94.4) *−6.1*[2]			•	135.1 *22.4*[7]					•
8-4[c]	•	128.4 *15.4*[5]									•	164.7 *9.5*[3]	•
8-6	•	135.8 *51.6*[15]									•	151.2 *9.4*[3]	•
8-8[d]	•	128.3 *33.5*[10]							•	132.9 *0.4*[0.1]	•	138.9 *7.8*[2]	•
8-10	•	117.2 *37.9*[12]							•	125.3 *1.2*[0.4]	•	130.8 *10.5*[3]	•
8-12	•	111.4 *74.7*[23]			(•	96.1 *−0.2*[0.1]			•	107.2) *−0.4*[0.1]	•	124.2 *12.1*[3]	•
8-14[e]	•	98.5 *45.6*[15]	(•	94.4) *−7.3*[2]			•	114.9 *3.0*[1]			•	118.9 *11.0*[3]	•

[a] Cr–Cr transition at 114 °C, ΔH = 0.8 kJ mol^{-1}. [b] Cr–Cr transition at 79 °C, ΔH = 59.7 kJ mol^{-1}. [c] Cr–Cr transition at 124 °C, ΔH = 27.6 kJ mol^{-1}. [d] Cr–Cr transition at 114 °C, ΔH = 0.5 kJ mol^{-1}. [e] Cr–Cr transition at 91 °C, ΔH = 85.5 kJ mol^{-1}.

phase according to Immirzi and Perini[13] gives a value of about 1.23 nm^3. Assuming a unit cell volume of 11.4 nm^3 calculated from the two-dimensional modulation parameters with the third dimension taken as the average repeating distance for neighbouring molecules estimated at 0.47 nm from the outer scattering, then there are, on average, 9.2 molecules in the unit cell, *i.e.* between 4 and 5 molecules within one block. These values correspond to a packing coefficient k = 0.7, a medium value in the crystalline state.[13,14] For the isotropic liquid with $k \approx 0.55$,[14] 3.6 molecules would fill the same volume of one block. Since the exact density of the compound in the SmÃ phase is not known we assume an intermediate value of about four molecules in the building block and eight molecules per unit cell. Approximately the same number results from a purely two-dimensional estimation. Thus, if the molecules are considered to be oriented parallel to the layer normal (in this case: along the *b*-axis) and the average lateral repeat distance is 0.47 nm (see above), then about 9.1 molecules are needed to fill the cell in the *a*-direction. The extension of the reflections

Table 2 Transition temperatures (°C), enthalpies (kJ mol^{-1}) in italics and the dimensionless value of $\Delta S/R$ in square brackets of homologues series **5-*n*** and **7-*n*** (B_6' denotes low temperature B_6 phase)

Dimer	Cr		B_6'		B_6		N_x		N		Iso
5-4	•	114.0 *49.5*[15]			(•	99.1 *−6.4*[2]			•	102.0) *−0.2*[0.1]	•
5-6	•	123.5 *63.8*[19]			(•	116.9) *−11.2*[3]					•
5-8	•	94.2 *56.8*[19]			•	121.0 *16.4*[5]					•
5-10	•	88.5 *54.4*[18]			•	109.5 *15.5*[5]					•
5-12	•	96.2 *78.6*[26]			(•	96.1) *−13.8*[5]					•
5-14	•	101.2 *104.0*[33]									•
7-4	•	112.2 *45.1*[14]			(•	84.4 *−2.5*[0.1]	•	96.6) *−0.5*[0.2]	•	115.0 *0.4*[0.1]	•
7-6[a]	•	96.4 *32.1*[10]			•	114.7 *12.5*[4]					•
7-8	•	111.2 *53.5*[17]			•	119.5 *17.1*[5]					•
7-10	•	100.1 *40.6*[13]	(•	93.7) *−0.2*[0.1]	•	110.1 *17.6*[6]					•
7-12	•	90.9 *63.7*[21]			•	99.3 *16.0*[5]					•
7-14[b]	•	73.3 *58.4*[19]									•

[a] Cr–Cr transition at 87.8 °C, ΔH = 1.7 kJ mol^{-1}. [b] Cr–Cr transition at 91 °C, ΔH = 8.0 kJ mol^{-1}.

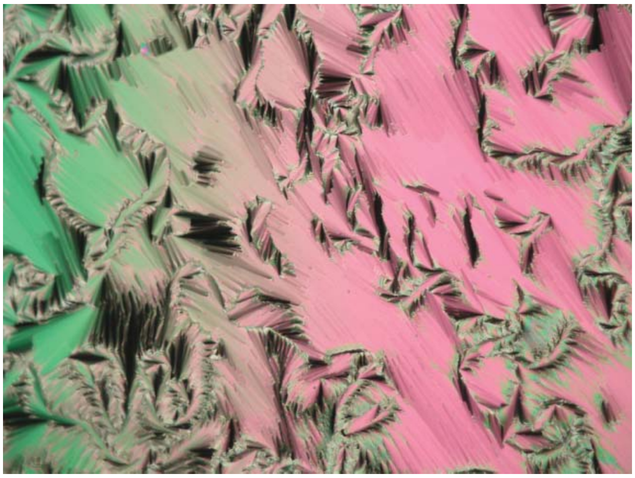

Fig. 2 Photomicrograph of the fan-like texture of the smectic Ã phase of **6-10** obtained at 112 °C.

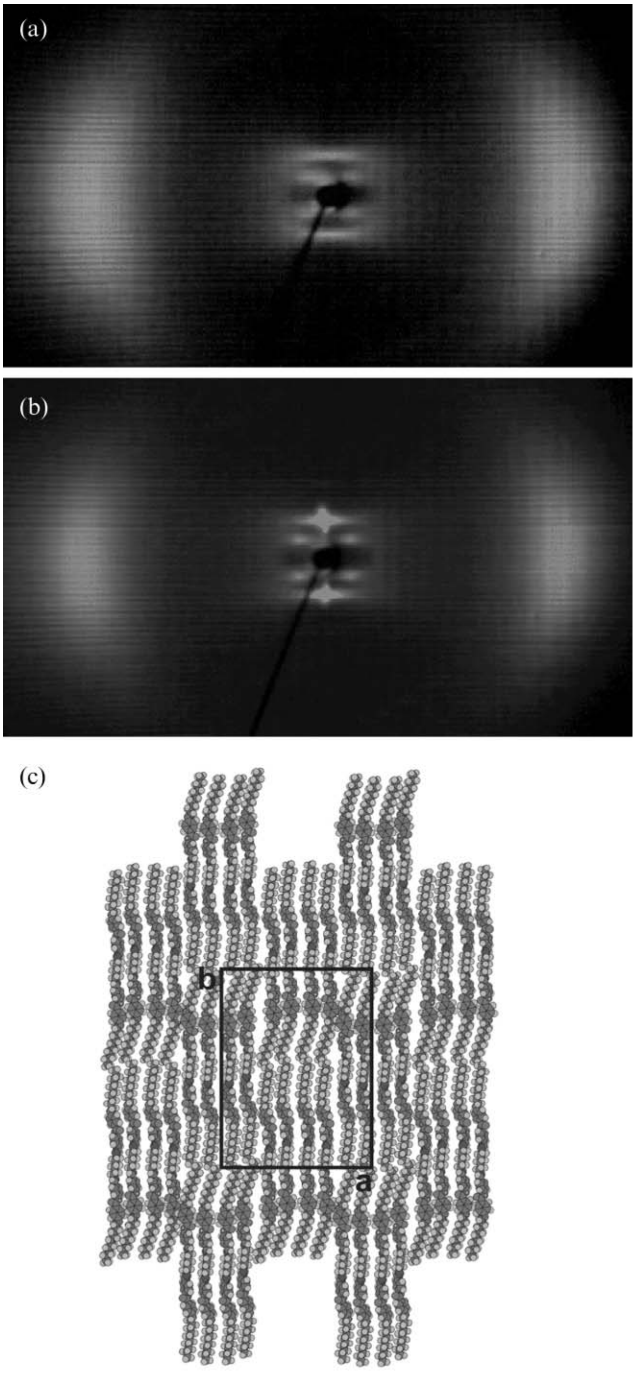

Fig. 3 X-Ray patterns of **6-10** aligned in the magnetic field on cooling from the isotropic liquid: a) nematic phase with cybotactic groups at 130 °C; b) Sm$\tilde{A}$ phase at 108 °C. c) Proposed molecular packing mode in the Sm$\tilde{A}$ phase of the dimers.

perpendicular to the layer normal shows that the correlation length in the *a*-direction is much smaller than that for the layers themselves, so that the order is probably only short-range. A model of the molecular packing in such a phase is given in Fig. 3c. The diffuse, small-angle scattering in the preceding nematic phase (Fig. 3a) can be attributed to cybotactic groups representing fluctuating arrays of molecules with a short-range order of the same type as the long-range order in the Sm$\tilde{A}$ phase.

Table 3 X-Ray data from Guinier powder patterns and from aligned samples (θ_{obs}: experimental scattering angle; d_{obs}: experimental *d* spacing; *n*/*hk*: assigned order of reflection/indices for 2D phases. Parameters: lattice parameters or *d* values with an error of the calculated parameters in the order of 0.1 nm, *L*: molecular lengths measured from CPK models, fully extended chains, zigzag shape for compounds with even-membered spacers, banana shape for those with odd-membered ones)

Compound	*T*/°C	Phase	θ_{obs}/°	d_{obs}/nm	*n*/*hk*	Parameter/nm	*L*/nm
6-10	108	Sm$\tilde{A}$	1.296	3.41	11	*a* = 4.27	5.8
			1.563	2.83	02	*b* = 5.66	
8-12	105	Sm$\tilde{A}$	1.100	4.01	11	*a* = 5.20	6.5
			1.400	3.15	02	*b* = 6.30	
6-12	110	SmC	1.112	3.97	1	*d* = 3.97	6.3
			2.225	1.98	2		
8-14	110	SmC	0.988	4.47	1	*d* = 4.47	6.9
			1.975	2.24	2		
5-8	105	B_6	1.888	2.34	1	*d* = 2.34	4.6
7-4	100	N	2.081[a]	2.12[a]			3.9
	88	N_x	2.148[a]	2.06[a]			
7-10	100	B_6	1.70	2.59	1	*d* = 2.59	5.0
	85	B_6'	1.68	2.62	1	*d* = 2.62	
7-12	96	B_6	1.60	2.76	1	*d* = 2.76	5.7

[a] For the maximum of the diffuse scattering in the small angle region.

For compound **8-12** the Sm$\tilde{A}$ phase was established based on a fan-shaped and a homeotropic texture. On cooling from the schlieren texture of the nematic phase, the Sm$\tilde{A}$ phase appeared as a fan-shaped texture. Further cooling results in a Sm$\tilde{A}$ to SmB transition, which can be recognised by the loss of fine details on the fluid fan texture on re-heating (Fig. 4).

As found already for compound **6-10**, X-ray measurements on **8-12** confirmed the formation of the Sm$\tilde{A}$ phase, the molecular length of about 6.5 nm as measured from CPK models being in good agreement with the cell parameter *b* = 6.3 nm in the direction of the long molecular axes (Fig. S1† and Table 3). From the same calculations as in the case of **6-10** an average number between 9.0 and 11.4 molecules per three-dimensional unit cell (molecular volume 20.0 nm^3 and 15.7 nm^3 for k = 0.55 and 0.7, respectively, and d = 0.48 for the wide-angle scattering) and 10.8 molecules per two-dimensional unit cell results for **8-12**. On cooling in real time an image of a pattern that could be attributed to a more ordered mesophase was observed for a short time on the monitor, but unfortunately, the alignment was lost and no recording was possible, because the sample rapidly crystallised, so a unique determination of the phase type was not possible from the X-ray patterns.

Compounds **6-12** and **8-14** display three different phase transitions. Enantiotropic N and SmC phases were identified according to their characteristic schlieren textures and, during transition from N to SmC, a typical fingerprint texture was observed. X-Ray measurements performed on both compounds showed the scattering typical of a nematic phase with cybotactic SmC groups on cooling when aligned in the magnetic field (Fig. 5, Fig. S2†). The measurements at 100 °C confirmed the presence of a SmC phase with molecules tilted strongly with respect to the layer normal (tilt angle 45° for **8-14**, see Fig. S3†).

Further cooling resulted in the appearance of a highly ordered monotropic phase whose texture depended strongly on

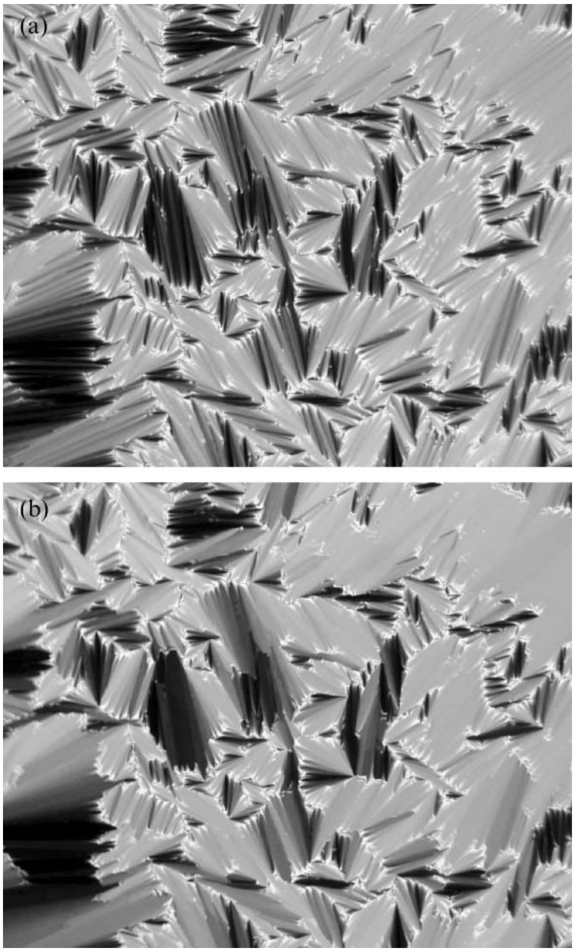

Fig. 4 Photomicrographs of compound **8-12** obtained on cooling: (a) fan-shaped texture of the SmÃ phase at 106 °C; (b) fan-shaped texture of the SmB phase at 96 °C.

the texture of the preceding SmC phase. Thus, on cooling, the monotropic phase appeared either as a mosaic texture if from a schlieren SmC texture (Fig. 6a and b) or as an arced, broken fan texture, if from a broken fan-shaped texture (Fig. 6c and d). As in the cases of **6-10** and **8-12**, rapid crystallisation prevented a clear recording of the X-ray diffraction pattern of these phases, but the textural behaviour in conjunction with the image of a highly ordered smectic phase observed for a short time during X-ray investigation (see Fig. S4†) implies the presence of a crystal G mesophase.

Compound **6-14**, in which the lengths of the chains are more than twice the length of the spacer, is the only compound that does not show a nematic phase. Instead, a direct transition from the isotropic liquid to a smectic C phase was observed. On cooling to a lower-temperature monotropic phase the schlieren texture transformed into a mosaic-like one while the broken fans became striped. The phase is again assigned as crystal G based on direct analogy with the textural behaviour displayed by compounds **6-10** and **8-14**.

Mesomorphism of 5-*n* and 7-*n*. Comparing to the even dimers the compounds with odd-numbered spacers (compounds **5-*n*** and **7-*n***) show completely different mesomorphic behaviour (Table 2).

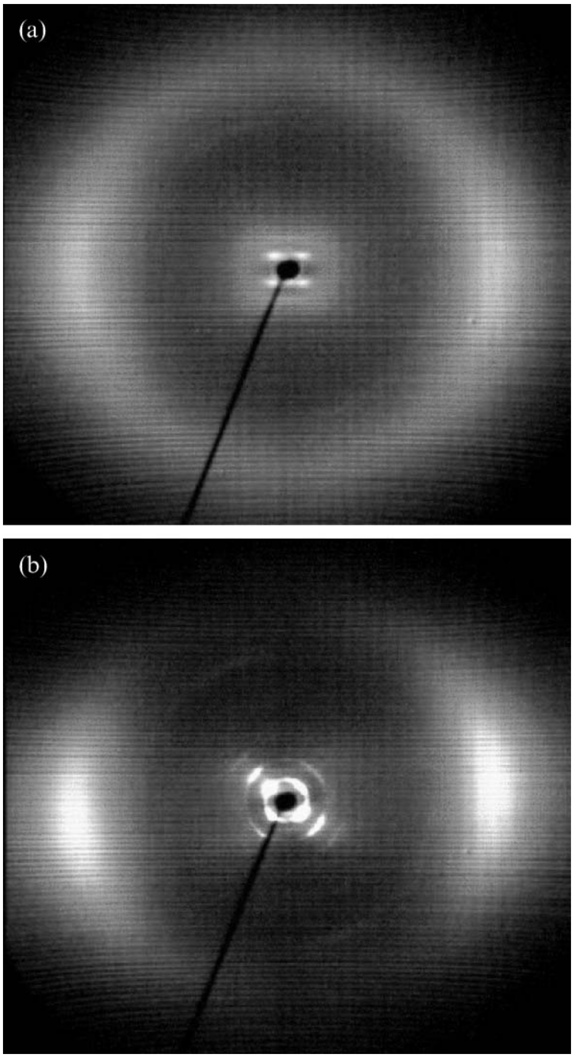

Fig. 5 X-Ray patterns of **8-14** aligned in the magnetic field on cooling from the isotropic liquid: a) nematic phase with cybotactic groups of the SmC type at 115 °C; b) SmC-type phase at 100 °C, the sample is fibre-like disordered around an axis parallel to the meridian of the pattern with one preferred orientation.

In both series, **5-*n*** and **7-*n***, a nematic phase was observed only for the shortest homologues, **5-4** and **7-4**. Microscopic observation of **5-4** revealed the presence of the nematic phase characterised by schlieren and marble textures. On further cooling the schlieren texture turned into fans without features characteristic of a N-to-SmA or a N-to-SmC transition. Applying mechanical stress resulted in a schlieren texture with two and four brushes. Similar textural characteristics were observed for the phases displayed by the higher homologues of both series and the miscibility studies performed by contact preparation reveal that they displayed the same phase. However, as the higher homologues do not exhibit a nematic phase this new liquid-crystalline phase separates out from the isotropic liquid in the form of bâtonnets which then coalescence and form a focal conic fan texture (Fig. 7a).

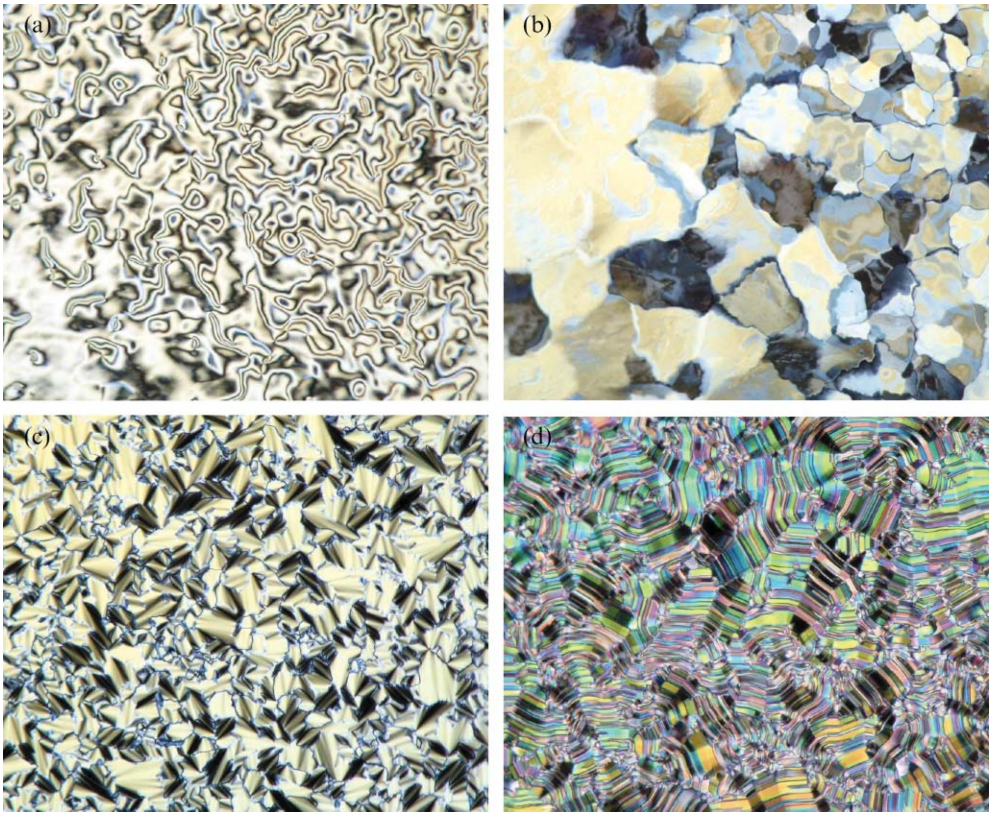

Fig. 6 Photomicrographs of compound **8-14** obtained on cooling: (a) schlieren texture of the SmC phase at 108 °C; (b) mosaic texture of the crystal G mesophase at 94 °C; (c) broken-fan texture of SmC phase at 96 °C; (d) arced-broken fan texture of the crystal G phase at 94 °C.

Shearing this specimen led again to a grey, schlieren-like texture with singularities of $S = \pm 1$ and $\pm ½$ (Fig. 7b) which have also been observed in antiferroelectric SmC,[15] intercalated SmC phases of mesogenic twins[2,4,7,16–18] or the B_6 phase of bent-core mesogens.[19,20] The occurrence of such singularities is attributed to an opposite tilt direction of the mesogenic groups between adjacent layers.[2,16,21]

In order to clarify the structure of this phase X-ray measurements were performed on compounds **5-8** and **7-10**. They showed very similar patterns for both compounds, as expected. Thus, layer reflections for the liquid-crystalline phase observed in the Guinier powder patterns at 2.34 nm for **5-8** and at 2.6 nm for **7-10** correspond to half the molecular length, suggesting an intercalated structure like B_6. The B_6 phase as described up to now in the literature is found to be tilted with a tilt angle of about 10–30° (tilt direction is perpendicular to the plane described by the bent-core molecules in the smectic layer).[19,20] Therefore aligned samples have been investigated, too (Fig. 8). In contrast to the alignment in the smectic phases of the even-membered compounds, the molecules adopted the so-called bookshelf orientation in this phase when surface aligned, which means that the layer normal is perpendicular to the meridian of the pattern and the layer reflections lie at the equator. The partially aligned samples showed the tilt angle to be small, below 15°. According to these X-ray patterns no unique choice can be made between the two possibilities of a small tilt or an orthogonal alignment, respectively. Microscopic observation showed that it was impossible to obtain a homeotropic texture either by shearing or by surface treatment, which implies a phase with tilted molecules, which can be characterised as a SmC_c phase.[22] Furthermore, the miscibility studies performed between the derivative of 1,3-diaminobenzene **1S**, for which a tilted, intercalated B_6 phase was established,[18] and homologue **7-8** showed continuous miscibility across the full composition range between **1S** and **7-8** for the B_6 phase, confirming that the odd dimers, indeed, display the B_6 phase, Fig. 9.

Thus, the B_6 phase is observed for all liquid-crystalline dimers with an odd-numbered alkylene spacer, the only exceptions being the highest homologues which show only a transition from crystal to isotropic liquid.

In addition to the already established nematic and B_6 phases, two homologues of series **7-*n*** display peculiar phase behaviour. Thus, the shortest homologue **7-4** has three different phases, displaying an enantiotropic nematic and two monotropic phases. On cooling from the isotropic liquid, the nematic phase showed typical marbled and homeotropic textures. Below this nematic were two monotropic phases and the transition to the higher-temperature of these was accompanied by a change in texture to a fan-like arrangement (Fig. 10a) that changed into oily streaks on shearing the sample (Fig. 10b). However, the intriguing parts of the fan-like texture are spiral domains whose origin we cannot currently explain (Fig. 10c), although we might speculate on whether this effect is related to escape from polar order, given the discussion below on the fairly strongly dipolar nature of these

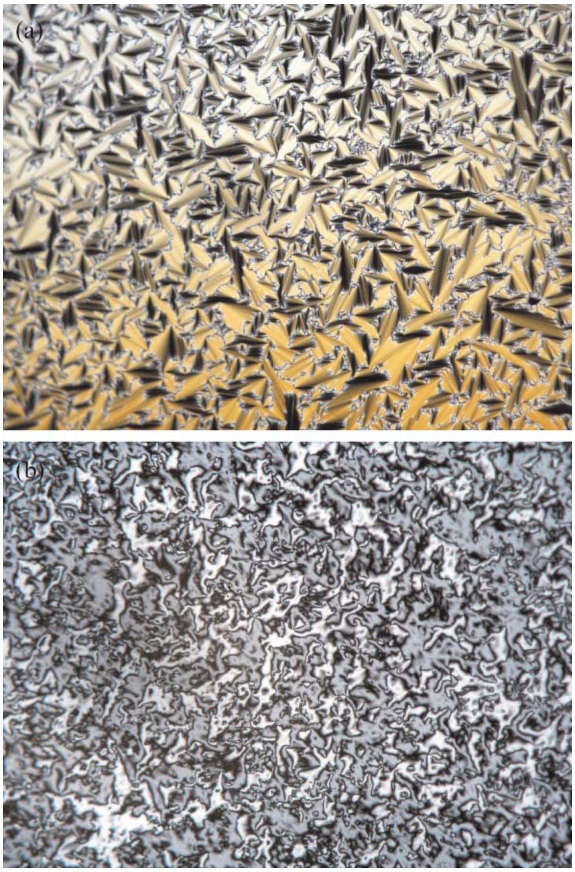

Fig. 7 Photomicrographs of compound **5-12**: (a) fan-like texture of the B6 phase; (b) schlieren-like texture of the B_6 phase obtained after shearing.

compounds. We also note in passing that Görtz and Goodby[23] recently reported spontaneous chiral separation in a phase below the nematic of some bent-core oxadiazole mesogens (although the optical textures were quite different) and that spontaneous symmetry breaking is a well-known phenomenon in certain phases of bent-core materials.[22]

The X-ray patterns show only diffuse scattering between ~107 and ~85 °C in a manner typical of nematic phases (Fig. 11). The temperature dependence of the position and width of the small-angle scattering measured on a powder-like sample with a position-sensitive detector gave only a weak indication of a phase transition between 92 and 96 °C on cooling (Fig. S5†), but the intensity and the position of this scattering with a maximum at d = 2.1 nm in the lower-temperature nematic phase (Fig. 11b) implies a correlation of the electron density maxima approximately orthogonal to the lateral distances of the molecules with short-range character. Although the textural behaviour resembles closely that observed previously for the N_{col} phase,[24,25] the d-value is only about half the molecular length, and the simple model of an N_{col} phase of bent-core mesogens cannot be applied.

The lower monotropic phase existed over a short temperature range and, again, during the X-ray investigation the sample crystallised. On cooling from N_x to this phase, very small fans developed that almost looked like a mosaic texture, Fig. 10d. However, on shearing the sample a schlieren-like texture with two and four brushes was observed, Fig. 10e. We believe, therefore, that the low-temperature, monotropic phase is the B_6 phase, identical to that displayed by the higher homologues of the same series. It is then interesting to speculate on whether the monotropic N_x phase can be regarded as a precursor of the B_6 phase, in which bundles of intercalated, bent-shaped molecules without long-range order are formed; this would be in line with the small enthalpy ($\Delta H = -2.47$ kJ mol^{-1}) for the N_x-to-B_6 transition.

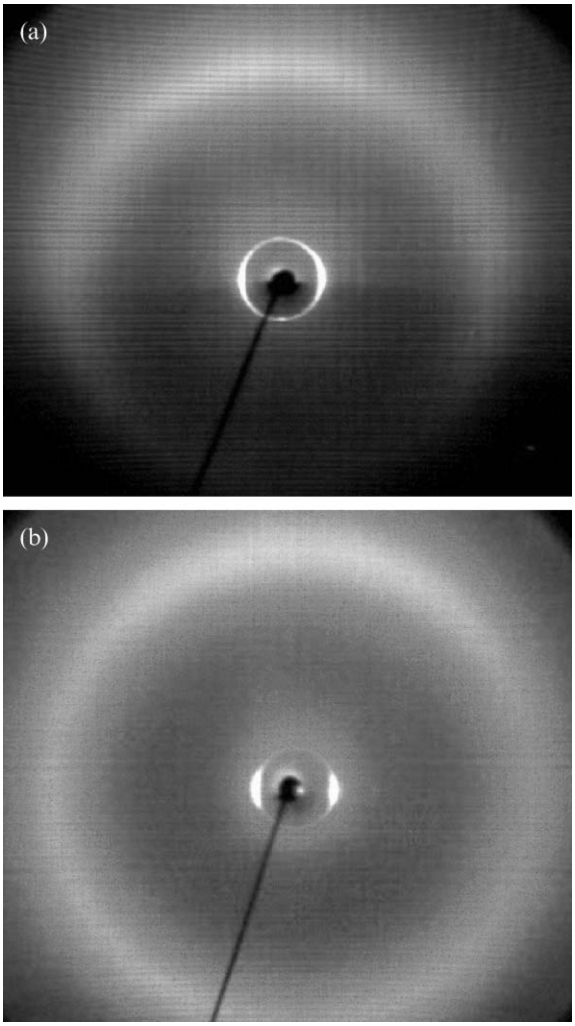

Fig. 8 X-Ray patterns of **5-8** and **7-10** partially aligned at the sample/air interface in the B_6-type phase on cooling: a) **5-8** at 111 °C; b) **7-10** at 100 °C.

Compound **7-10** is the only dimer with an odd number of methylenes in the spacer to display smectic polymorphism and the DSC trace of **7-10** revealed the presence of two mesophases. Combination of the microscopic observations and X-ray measurements revealed that the high-temperature, enantiotropic mesophase is the B_6 phase (Fig. 8b). The low-temperature monotropic phase occurred during the cooling cycle at 93.7 °C and the transition was accompanied by a small change in enthalpy of -0.24 kJ mol^{-1}. The phase showed a focal-conic fan texture crossed with light bands and a schlieren texture (Fig. 12c and d). The X-ray measurements did not show any significant change in the temperature dependence of

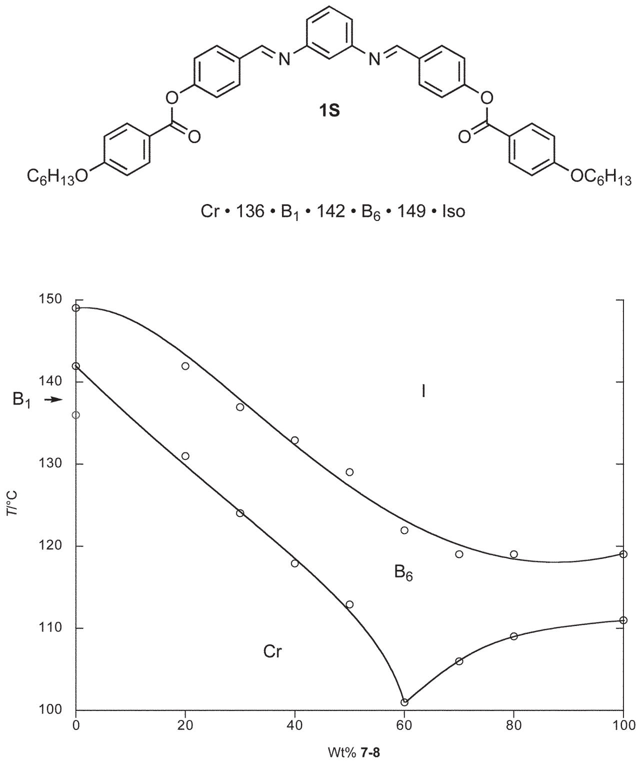

Fig. 9 Miscibility phase diagram between **1S** and **7-8**.

the layer distance on cooling, including at the transition from the B_6 to the lower-temperature mesophase and indeed until the sample crystallised (Fig. S6†). On the other hand, the appearance of second- and third-order layer reflections in the lower temperature phase (Fig. 13) suggests a change in the quasi-long range order from a sinusoidal modulation of the electron density along the layer normal found in the higher temperature phase (where only the first order is observed), to more strictly defined layers with a more pronounced segregation of the aromatic and aliphatic parts of the molecules within the intercalated structure. The small enthalpy change of -0.24 kJ mol^{-1} is in agreement with such a small change in the molecular arrangement and its non-zero value allows for a transition with no change in overall symmetry. In Table 2, the high- and the low-temperature mesophases are assigned as B_6 and B_6' respectively.

The results presented above show a remarkable effect of the imino linkage group as well as of the chain length and the spacer parity on the mesomorphic behaviour. The compounds with an even number of methylene units in the spacer display mesomorphism in accordance with their overall linear shape. A comparison of the mesomorphic behaviour of the series **6-*n*** and **8-*n*** (Table 1) reveals that the nature of the phase formed strongly depends on the ratio between the length of the terminal chain and the length of the spacer (n/m).

Thus, all the compounds of the series **6-*n*** and **8-*n***, except **6-14** for which $n/m > 2$, show nematic phases. Among these, for the compounds with $n/m \leqslant 1$ only the nematic phase was observed. Increasing the terminal alkoxy chain resulted in the appearance of an additional smectic phase and the smectic polymorphism. Thus, the Sm$\tilde{\mathrm{A}}$ phase was found for the ratio $1 \leqslant n/m \leqslant 1.6$, while a further increase in the ratio ($n/m > 1.7$) resulted in the observation of SmC and crystal G phases. An intercalated SmA$_c$ phase in which the molecules are arranged in such a way that the spacer and terminal chains are mixed randomly was observed for the even symmetric dimers having terminal chains equal to or shorter than the spacer.[7] The presence of an intercalated layer structure has been explained

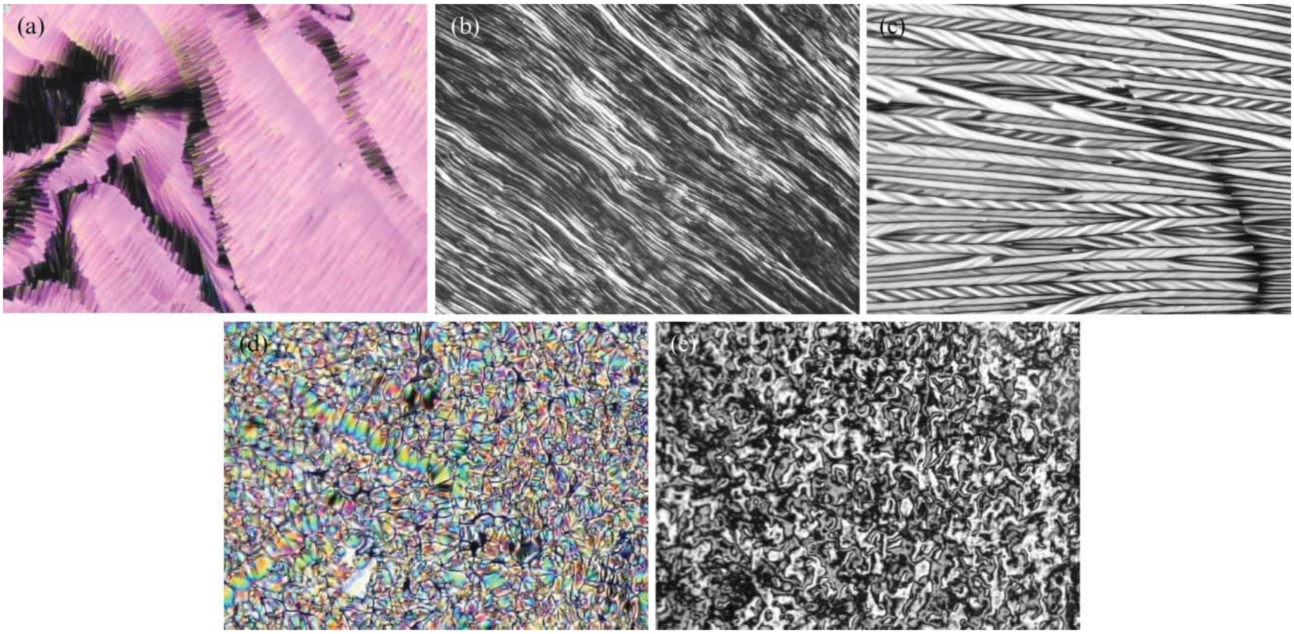

Fig. 10 Photomicrographs of compound **7-4**: (a) fan-like texture of the monotropic high-temperature phase; (b) oily streaks texture of the monotropic high-temperature phase obtained after shearing the fan-like texture; (c) texture of the monotropic high-temperature phase containing spiral domains with both handednesses; (d) fan-like texture of the monotropic low-temperature phase; (e) schlieren-like texture of the monotropic low-temperature phase.

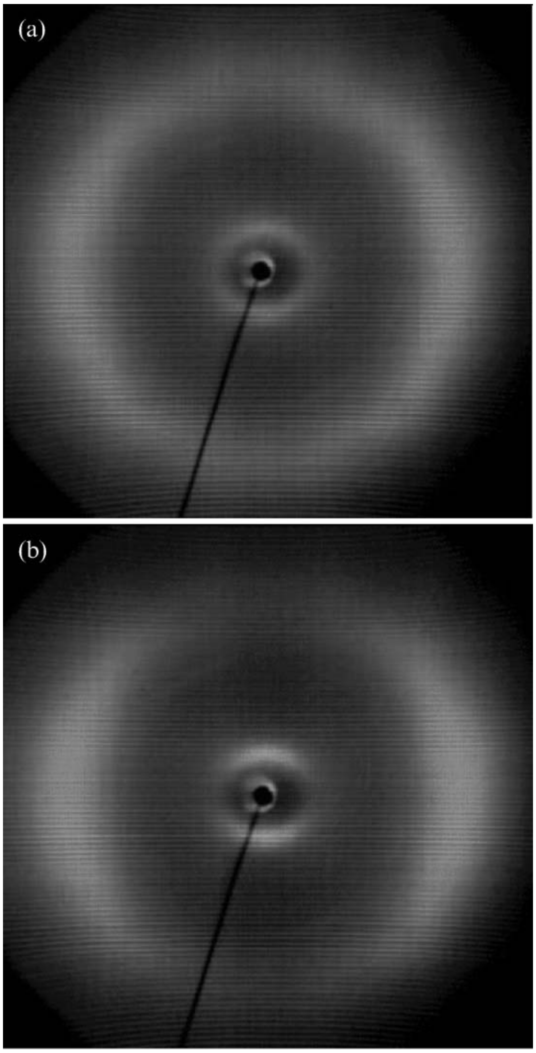

Fig. 11 X-Ray patterns of **7-4** aligned in the magnetic field on cooling from the isotropic liquid: a) N phase at 100 °C, b) the lower temperature nematic phase at 90 °C.

previously in terms of either an electrostatic, quadrupolar interaction, an increase in entropy gained from the homogeneous mixing of the mesogenic moieties, or by excluded-volume or space-filling constraints.[4] In our case, the length of the terminal chains exceeds the length of the spacer, and the splitting of the layers into blocks with a width of only a few molecules in a non-intercalated SmA arrangement and SmA_c interfaces implies the presence of strong, lateral interactions between the mesogenic units that compete with unfavourable, space-filling interactions caused by a mismatch in the lengths of the chains and the spacer. Increasing n/m beyond 1.7 enhances unfavourable interactions caused by the inability of the spacer to accommodate two, long chains and destabilises the intercalated arrangement. As a result, the molecules segregate into a non-intercalated smectic phase containing three, distinct regions: mesogenic units, spacers and terminal alkoxy chains.

The tendency toward intercalation is even more pronounced for the dimers with an odd-numbered spacer. Contrary to expectations, the mesomorphic behaviour of these dimers appears almost insensitive to the chain length and all except the highest homologues display the intercalated B_6 phase. This phase persists until the chains become nearly twice the length of the spacer and then, instead of forming the segregated non-intercalated structures, the liquid crystallinity is lost. In addition to the B_6 phase, only the lowest odd homologues display a nematic phase.

A comparison of the thermodynamic data between the lowest homologues (n = 4) of each series reveals a strong odd–even effect. According to the model developed by Luckhurst *et al.*,[26] the magnitude of the effect depends strongly on the nature of the link between the mesogenic unit and the alkylene spacer and, with increasing molecular biaxiality, the value of $\Delta S_{NI}/R$ decreases. The very tiny values of $\Delta S_{NI}/R$ observed here point to the presence of a highly bent conformer whose geometry is imposed by the imino linkage group and odd parity of the spacer. Therefore, the dimers with odd-numbered spacers described here can be regarded as true, bent-shaped molecules that display a 'B-type' phase characteristic for bent-core molecules containing a rigid angular central unit.

The results presented above show that the dimers described here display strong affinity for intercalated structures regardless of the spacer parity and it has been suggested that a specific, dipolar interaction is required between two mesogenic groups in order to stabilise the intercalated arrangement.[27] In consideration of this hypothesis, we carried out gas-phase electronic structure calculations using density functional theory[28] with the B1LYP functional[29,30] and the 6-31G(d,p) basis set on the model compound, **M** (Fig. 14), that represents one half of a dimer.

Since the most critical fragment in the structure is the ester linkage, we performed a calculation of the energy as a function of the dihedral angle (ϕ) C1–C2–O3–C4. The results revealed that the molecule has a great degree of rotational freedom having the rotational barriers within 5 kJ mol^{-1}. Rotation around the C2–O3 bond gives two shallow minima that differ in energy by only 1.3 kJ mol^{-1}. Both minima correspond to the geometry in which the phenyl ring can make any angle within 30° with the plane of the benzoate group without significant increase in energy. However, according to the energy content, the conformer having the dihedral angle $\phi = 180°$ is more stable than the conformer where $\phi = 10°$. As a result of different dihedral angles, the geometries of the conformers can be distinguished by the directions of the carbonyl and imino groups relative to one another and these can plausibly be assigned as *anti* for the former and *syn* for the latter. The calculation of dipole moment for each conformer revealed that the total dipole moment for the twisted, *syn* conformer (3.34 D) is much higher than for the planar, *anti* conformer (2.69 D). In addition, the results shows that the dipole origin is in the mass centre of the molecule and points toward the imino linkage group at an angle of 34°, as a consequence of which the strongest contribution is along the x-axis, which is parallel to the principal axis of the molecule (Fig. 15).

From the experimental data for the odd dimers (**5-*n*** and **7-*n***), the layer distance that corresponds to $1/2L$ of the highly bent conformer and very tiny values of $\Delta S_{NI}/R$ point strongly to the presence of the *syn* conformer in the liquid-crystalline

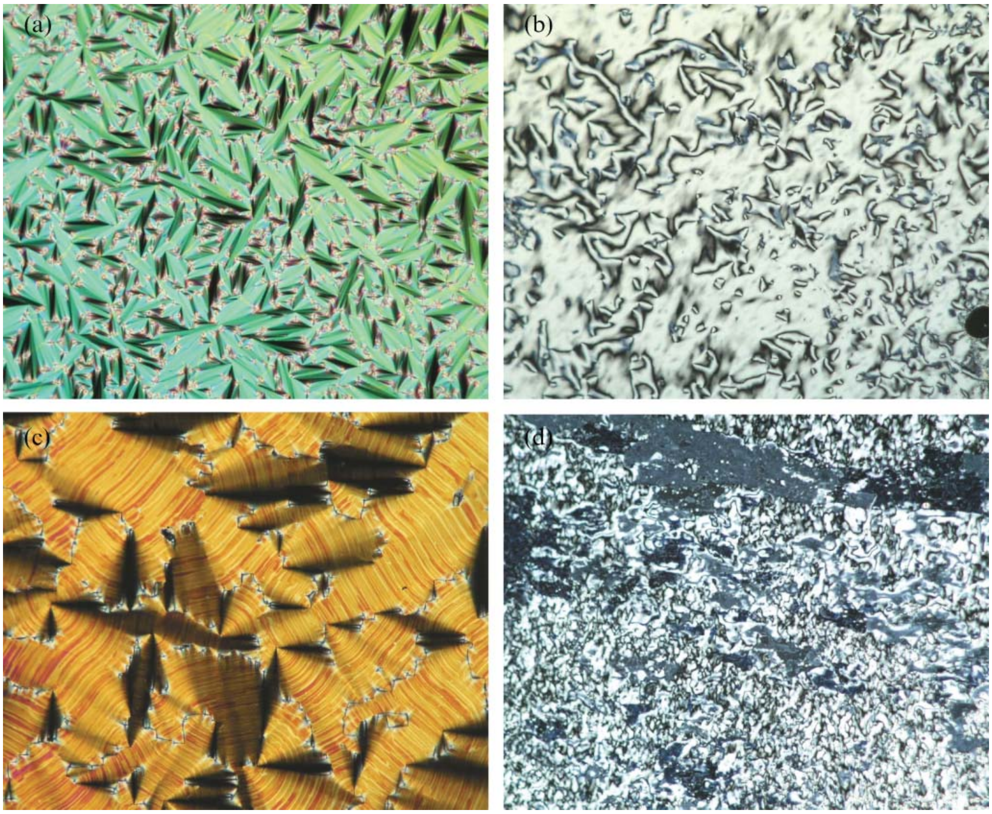

Fig. 12 Photomicrographs of compound **7-10**: (a) fan-like texture of the B_6 phase; (b) schlieren-like texture of the B_6 phase; (c) focal-conic fan texture of the monotropic B_6' phase; (d) schlieren-like texture of the monotropic B_6' phase.

state and, consequently, to stronger dipole–dipole interactions. Taking into account more than one molecule in the side-by-side arrangement, the electrostatic repulsion between two dipoles is minimised by their antiparallel orientation. Application of this model to the layer arrangement of the dimeric molecules indicates strongly that the compensation of the dipoles is a driving force for the formation of an intercalated structure.

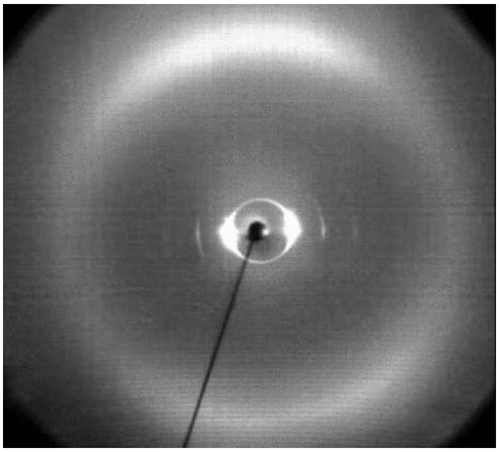

Fig. 13 X-Ray pattern of **7-10** partially aligned at the sample/air interface in the low-temperature B_6' phase at 81 °C on cooling.

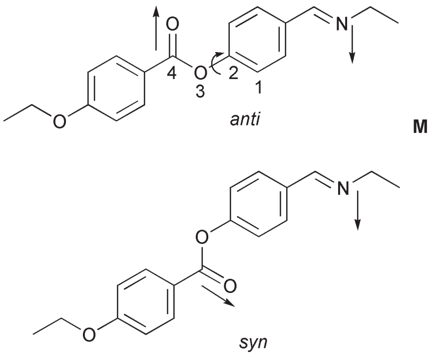

Fig. 14 Half-dimer molecule **M** used in the DFT calculations.

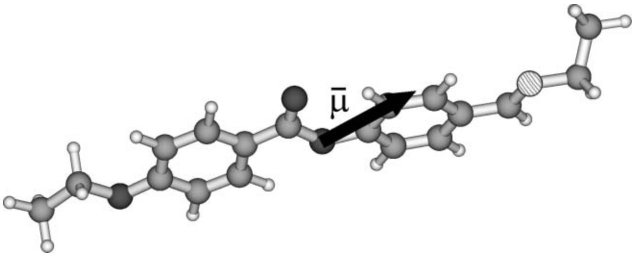

Fig. 15 Ball-and-stick presentation of the *syn* conformer obtained from electronic structure calculations showing the projection of the dipole moment (arrow).

Conclusion

Here we have described the synthesis and the mesomorphic properties of four series of dimeric molecules in which the benzoyloxybenzylidene groups are linked to an alkylene spacer *via* an imino group. In order to study structure–property relationships, the lengths of the alkylene spacers (m = 5 to 8) as well as those of the terminal alkoxy chains (n = 4 to 14) have been varied. The results show that both the spacer parity and the imino linkage have a great impact on the mesomorphic behaviour. Furthermore, the influence of the chain length on the liquid-crystalline properties is much more pronounced for the even compared to the odd dimers. The even dimers exhibit both modulated and non-intercalated structures depending on the n/m ratio, while the odd ones display an intercalated B_6 phase with the exception of homologues with n = 14.

Quantum chemical calculations on the model compound suggest that the compensation of the dipoles is responsible for forming the intercalated structures. The presence of the intercalated phase in the dimers of both spacer parities at high n/m ratios indicates that the antiparallel arrangement of the molecules within the phase is facilitated by strong, dipole–dipole interactions between mesogenic units, which appear to prevail over unfavourable, space-filling interactions caused by a mismatch in the lengths of the chains and the spacer. Furthermore, the imino linkage group coupled with an odd spacer parity gives rise to the highly bent geometry of the molecules, causing the odd dimers to behave like true bent-core mesogens.

Thus, our studies reveal that the imino-linkage group takes a significant part in the generation of dipolar interactions favouring intercalated structures and, in conjunction with the spacer parity, dictating the geometry of the dimer. As such, it has an important rôle in the determination of the liquid-crystalline behaviour.

Experimental

All the solvents were either *puriss p.a.* quality or distilled over appropriate drying reagents.[31] All the other reagents were used as purchased from Aldrich. ^{1}H- (300 MHz) and ^{13}C- (75.5 MHz) NMR spectra were recorded on a Bruker AV 300 instrument in $CDCl_3$ with $SiMe_4$ as internal standard unless stated otherwise. Infrared spectra were recorded on a Bomem MB 102 spectrophotometer; absorption maxima are given in cm^{-1}. Phase transition temperatures and textures were determined using an Olympus BX51 polarizing microscope equipped with a Linkam TH600 hot stage and a PR600 temperature controller. Enthalpies of transition were determined from thermograms recorded on a Perkin-Elmer DSC-7 differential scanning calorimeter operated at scanning rates of 5 to 10 K min^{-1}. Powder X-ray patterns were obtained with a Guinier film camera (HUBER Diffraktionstechnik, Germany) using quartz-monochromated CuK$_\alpha$ radiation and, for the small-angle region, with a modified Kratky camera and a one-dimensional position-sensitive detector (M. Braun, Germany) using Ni-filtered CuK$_\alpha$ radiation from samples in glass capillaries (diameter 1 mm) mounted in temperature-controlled heating stages. Patterns of aligned samples on a glass plate on a temperature-controlled heating stage (alignment at the sample/glass or at the sample/air interface, sample fibre-like disordered around an ∞-fold axis perpendicular to this interface) were obtained with a two-dimensional detector (HI-STAR, Siemens).

General procedure for the preparation of imines

A solution of the appropriate α,ω-diamine (1 mmol) in ethanol (absolute, 5 cm^3) was added dropwise to a hot solution of the corresponding aldehyde (**3a–f**; 2 mmol) in ethanol (absolute, 25 cm^3). The reaction mixture was heated under reflux for 1 h under argon and then cooled to room temperature. The crystalline product, which precipitated, was separated by filtration. The pure product was obtained after several crystallisations from acetone or toluene in yields of 60 to 80%.

Analytical data for the new dimeric compounds are collected in Table 4. Spectroscopic data are given for one imine homologue, since the only significant difference in the NMR spectra relates to the number of carbons in the alkoxy chains and alkylene spacer.

***N*,*N*′-Bis[4′-(4″-decyloxybenzoyloxy)benzylidene]heptane-1,7-diamine 7-10.** IR (KBr) ν(cm^{-1}): 2921, 1725, 1648, 1607, 1262; ^{1}H-NMR ($CDCl_3$) δ: 0.89 (t, J = 6.6 Hz, 6H), 1.04–1.85 (m, 42H), 3.62 (t, J = 6.6 Hz, 4H), 4.05 (t, J = 6.6 Hz, 4H –OCH_2), 6.98 (d, J = 8.7 Hz, 4H Ar), 7.26 (d, J = 8.4 Hz, 4H Ar), 7.79 (d, J = 8.4 Hz, 4H Ar), 8.14 (d, J = 8.7 Hz, 4H Ar), 8.28 (s, 2H CH=N); ^{13}C-NMR ($CDCl_3$) δ: 14.01, 22.57, 25.85,

Table 4 Analytical data for the new, dimeric compounds

Dimer	Analysis: Calc (Found) (%) C	H	N	Dimer	Analysis: Calc (Found) (%) C	H	N
5-4	74.3 (74.2)	7.0 (7.3)	4.2 (4.3)	**6-4**	74.5 (74.6)	7.2 (7.3)	4.1 (4.2)
5-6	75.2 (75.3)	7.6 (7.7)	3.9 (4.0)	**6-6**	75.4 (75.3)	7.7 (7.8)	3.8 (3.9)
5-8	75.9 (75.9)	8.1 (8.1)	3.6 (3.6)	**6-8**	76.1 (75.9)	8.2 (8.2)	3.6 (3.6)
5-10	76.6 (76.3)	8.5 (8.4)	3.4 (3.4)	**6-10**	76.7 (76.7)	8.6 (8.8)	3.3 (3.5)
5-12	77.2 (77.4)	8.9 (9.1)	3.1 (2.9)	**6-12**	77.3 (77.2)	9.0 (9.0)	3.1 (3.2)
5-14	77.7 (77.7)	9.2 (9.1)	3.0 (3.0)	**6-14**	77.8 (77.8)	9.3 (9.2)	2.9 (3.0)
7-4	74.8 (74.6)	7.3 (7.5)	4.1 (4.1)	**8-4**	75.0 (74.9)	7.4 (7.6)	4.0 (4.0)
7-6	75.6 (75.7)	7.8 (7.8)	3.8 (3.5)	**8-6**	75.8 (76.0)	8.0 (7.9)	3.7 (3.6)
7-8	76.3 (76.6)	8.3 (8.5)	3.5 (3.4)	**8-8**	76.4 (76.6)	8.4 (8.6)	3.4 (3.4)
7-10	76.9 (77.1)	8.7 (8.9)	3.3 (3.1)	**8-10**	77.0 (77.1)	8.8 (9.0)	3.2 (3.3)
7-12	77.4 (77.6)	9.0 (9.2)	3.1 (3.1)	**8-12**	77.6 (77.3)	9.1 (9.3)	3.0 (3.0)
7-14	77.9 (78.1)	9.3 (9.5)	2.9 (3.0)	**8-14**	78.0 (78.0)	9.4 (9.7)	2.8 (2.6)

27.16, 28.98, 29.11, 29.25, 29.44, 30.73, 31.78, 61.61, 68.22, 114.18, 121.17, 121.89, 129.03, 132.19, 133.77, 152.62, 159.57, 163.49, 164.55.

Acknowledgements

The authors would like to thank the UK EPSRC (HLN) and the MZOS Republic of Croatia for financial support, and the Royal Society of London for the provision of a Collaborative Grant that facilitated the collaboration between AL and DWB. We are also grateful to Dr Nađa Došlić (Ruđer Bošković Institute, Zagreb) for performing the electronic structure calculations and Professor John Goodby (University of York) for helpful discussions concerning optical textures.

References

1 A. C. Griffin and T. R. Britt, *J. Am. Chem. Soc.*, 1981, **103**, 4957.
2 G. S. Attard, R. W. Date, C. T. Imrie, G. R. Luckhurst, S. J. Roskilly, J. M. Seddon and L. Taylor, *Liq. Cryst.*, 1994, **16**, 529.
3 C. T. Imrie and G. W. Luckhurst, in *Handbook of Liquid Crystals*, ed. D. Demus, J. W. Goodby, G. W. Gray, H.-W. Spiess and V. Vill, Wiley-VCH, Weinheim, 1998, vol. 2B, ch. X.
4 C. T. Imrie and P. A. Henderson, *Curr. Opin. Colloid Interface Sci.*, 2002, **7**, 298 and references therein.
5 P. A. Henderson, J. M. Seddon and C. T. Imrie, *Liq. Cryst.*, 2005, **32**, 1499.
6 C. T. Imrie, *Struct. Bonding*, 1999, **95**, 149.
7 J. Watanabe, H. Komura and T. Niiori, *Liq. Cryst.*, 1993, **13**, 455.
8 S. W. Choi, M. Zennyoi, Y. Takanishi, H. Takazoe, T. Niori and J. Watanabe, *Mol. Cryst. Liq. Cryst.*, 1999, **328**, 185.
9 J. Watanabe, T. Izumi, T. Niori, M. Zennyoji, Y. Takanishi and H. Takezoe, *Mol. Cryst. Liq. Cryst.*, 2000, **346**, 77.
10 J. Watanabe, T. Niori, S.-W. Choi, Y. Takanishi and H. Takezoe, *Jpn. J. Appl. Phys., Part 2*, 1998, **37**, L401.
11 M. Šepelj, A. Lesac, U. Baumeister, S. Diele, D. W. Bruce and Z. Hameršak, *Chem. Mater.*, 2006, **18**, 2050.
12 D. Demus and H. Sackmann, *Z. Phys. Chem. (Leipzig)*, 1963, **222**, 127. Phase sequence in °C of ethyl-(*p*-ethoxybenzal)-*p*-aminocinnammate: Cr 77.1 SmB 115.6 SmA 155.4 N 157.6 I.
13 A. Immirzi and B. Perini, *Acta Crystallogr., Sect. A*, 1977, **33**, 216.
14 A. I. Kitaigorodski, *Molekülkristalle*, Akademieverlag Berlin, 1979.
15 Y. Takanishi, H. Takezoe, A. Fukuda, H. Komura and J. Watanabe, *J. Mater. Chem.*, 1992, **2**, 71.
16 W. Weissflog, C. Lischka, K. Pelzl, I. Wirth, S. Diele and G. Pelzl, *Mol. Cryst. Liq. Cryst.*, 2001, **364**, 279.
17 C. V. Yelamaggad, S. Anitha Nagamani, U. S. Hiremath, D. S. Shankar Rao and S. Krishna Prasad, *Liq. Cryst.*, 2002, **29**, 1401.
18 R. Achten, A. Koudijs, Z. Karczmarzyk, A. T. M. Marcelis and E. J. R. Sudholter, *Liq. Cryst.*, 2004, **31**, 215.
19 W. Weissflog, I. Wirth, S. Diele, G. Pelzl, T. Schmalfuss, A. Schoss and H. Würflinger, *Liq. Cryst.*, 2001, **28**, 1603.
20 J. C. Rouillon, J. P. Marcerou, M. Laguerre, H. T. Nguyen and M. F. Achard, *J. Mater. Chem.*, 2001, **11**, 2946.
21 J. Watanabe and S. Kinoshita, *J. Phys. II*, 1995, **2**, 1237.
22 R. A. Reddy and C. Tschierske, *J. Mater. Chem.*, 2006, **16**, 907.
23 V. Görtz and J. W. Goodby, *Chem. Commun.*, 2005, 3262.
24 M. W. Schröder, S. Diele, G. Pelzl, U. Dunemann, H. Kresse and W. Weissflog, *J. Mater. Chem.*, 2003, **13**, 1877.
25 A. Lesac, H. L. Nguyen, S. Narančić, U. Baumeister, S. Diele and S. D. W. Bruce, *Liq. Cryst.*, 2006, **33**, 167.
26 A. Ferrarini, G. R. Luckhurst, P. L. Nordio and S. J. Roskilly, *Liq. Cryst.*, 1996, **21**, 373.
27 A. E. Blatch and G. R. Luckhurst, *Liq. Cryst.*, 2000, **27**, 775.
28 M. J. Frisch, G. W. Trucks, H. B. Schlegel, G. E. Scuseria, M. A. Robb, J. R. Cheeseman, J. A. Montgomery, Jr., T. Vreven, K. N. Kudin, J. C. Burant, J. M. Millam, S. S. Iyengar, J. Tomasi, V. Barone, B. Mennucci, M. Cossi, G. Scalmani, N. Rega, G. A. Petersson, H. Nakatsuji, M. Hada, M. Ehara, K. Toyota, R. Fukuda, J. Hasegawa, M. Ishida, T. Nakajima, Y. Honda, O. Kitao, H. Nakai, M. Klene, X. Li, J. E. Knox, H. P. Hratchian, J. B. Cross, V. Bakken, C. Adamo, J. Jaramillo, R. Gomperts, R. E. Stratmann, O. Yazyev, A. J. Austin, R. Cammi, C. Pomelli, J. Ochterski, P. Y. Ayala, K. Morokuma, G. A. Voth, P. Salvador, J. J. Dannenberg, V. G. Zakrzewski, S. Dapprich, A. D. Daniels, M. C. Strain, O. Farkas, D. K. Malick, A. D. Rabuck, K. Raghavachari, J. B. Foresman, J. V. Ortiz, Q. Cui, A. G. Baboul, S. Clifford, J. Cioslowski, B. B. Stefanov, G. Liu, A. Liashenko, P. Piskorz, I. Komaromi, R. L. Martin, D. J. Fox, T. Keith, M. A. Al-Laham, C. Y. Peng, A. Nanayakkara, M. Challacombe, P. M. W. Gill, B. G. Johnson, W. Chen, M. W. Wong, C. Gonzalez and J. A. Pople, *GAUSSIAN 03 (Revision B.05)*, Gaussian, Inc., Pittsburgh, PA, 2003.
29 C. Adamo and V. Barone, *Chem. Phys. Lett.*, 1997, **274**, 242.
30 N. Došlić, J. Stare and J. Mavri, *Chem. Phys.*, 2001, **269**, 53.
31 D. D. Perrin, W. L. F. Armarego, D. R. Perrin and C. Chai, *Purification of Laboratory Chemicals*, Butterworth, London, 2003.